



## Regular article

# Evaluation of inhibition of lignocellulose-derived by-products on bioethanol production by using the QSAR method and mechanism study

Jinju Hou<sup>a</sup>, Jiawen Tang<sup>a</sup>, Jinhuan Chen<sup>a</sup>, Jie Deng<sup>a</sup>, Juan Wang<sup>a,\*</sup>, Qiuzhuo Zhang<sup>a,b,\*</sup>

<sup>a</sup> Shanghai Key Lab for Urban Ecological Processes and Eco-Restoration, School of Ecological and Environmental Sciences, East China Normal University, 200241, Shanghai, China

<sup>b</sup> Institute of Eco-Chongming (IEC), 3663 N. Zhongshan Rd., Shanghai, 200062, China

## HIGHLIGHTS

- Inhibition of by-products existed in lignocellulose hydrolysates was investigated.
- QSAR models were successfully established for evaluating the inhibition effects.
- Strong relationship was found between molecular descriptors and inhibition effects.
- Ferulic acid played a key role for combined inhibitions of binary mixtures.

## ARTICLE INFO

## Keywords:

Inhibitors  
Fermentation inhibition  
Bioethanol  
QSAR

## ABSTRACT

To evaluate the inhibition of by-products that exist in pretreated lignocellulose hydrolysate on bioethanol fermentation, quantitative structure-activity relationship (QSAR) models were established in the present study. These models have the potential to predict the fermentation inhibition to minimize the experimental effort. They also provided an innovative methodology for removing fermentation inhibitors purposefully and for optimizing pretreatment parameters and thus could enhance the bioethanol yield. The results indicated that the fermentation inhibition of phenolic aldehyde were stronger than that of phenolic acid followed by phenolic alcohol in which the fermentation inhibition was weakened by the existence of the methoxy group in the benzene ring. Meanwhile, the formation of the intramolecular hydrogen bonds of fermentation inhibitors also played an important role in weakening their fermentation inhibition. The individual fermentation inhibition of fermentation inhibitors was found strongly related to their molecular descriptors. Furthermore, ferulic acid was chosen as the representative inhibitor for the primary investigation on the combined fermentation inhibition of the various complex binary fermentation inhibitor mixtures, which co-existed in the lignocellulose hydrolysate. As indicated by the results, antagonism occurred mainly under the higher ferulic acid concentrations in the binary mixtures, while a simple additive effect was generated.

## 1. Introduction

Owing to the rising concern over the energy crisis and climate change, the development of alternative clean energy sources is drawing more attention [1,2]. Bioethanol, which is produced from abundant non-food lignocellulose biomass, is considered as one of the most promising renewable energies currently, due to its environmentally friendly nature, low cost of raw material and abundant reservation [3,4]. To convert the lignocellulose biomass into bioethanol efficiently, the pretreatment of feedstocks is crucial, which could facilitate the

decomposition of stable lignocellulose structures into soluble sugars, thus improving the bioethanol yield [5,6]. However, a large amount of lignocellulose-derived fermentation by-products will be generated during this process, thereby inhibiting the subsequent biochemical processes [7,8]. Therefore, it is of great significance to investigate these fermentation inhibitors.

The fermentation inhibitors are divided into three main groups, including phenolic compounds, furan derivatives and weak acids, which originated from the hydrolysis of lignin, sugar and pretreated lignocellulose degradation compounds, respectively [9,10]. The

\* Corresponding authors at: Shanghai Key Lab for Urban Ecological Processes and Eco-Restoration, School of Ecological and Environmental Sciences, East China Normal University, 200241, Shanghai, China.

E-mail addresses: [jwang@re.ecnu.edu.cn](mailto:jwang@re.ecnu.edu.cn) (J. Wang), [qzhang@des.ecnu.edu.cn](mailto:qzhang@des.ecnu.edu.cn) (Q. Zhang).

<https://doi.org/10.1016/j.bej.2019.04.013>

Received 7 January 2019; Received in revised form 28 March 2019; Accepted 14 April 2019

Available online 16 April 2019

1369-703X/ © 2019 Elsevier B.V. All rights reserved.

## Nomenclatures

QSAR	Quantitative structure-activity relationship
<i>S. cerevisiae</i>	<i>Saccharomyces cerevisiae</i>
5-HMF	5-hydroxymethylfurfural
CICC	China center of industrial culture collection
YPG	Yeast peptone glucose medium
OD <sub>600</sub>	Optical density at 600 nm
UV/Vis	Ultraviolet-visible spectrophotometry
GC	Gas chromatography
VIAL	Headspace vial temperature
LOOP	Coil temperature
TR. LINE	Conveyor belt temperature
VIALEQ.TIME	Headspace vial equilibration time
Q	Ethanol productivity with fermentation inhibitors
Q <sub>c</sub>	Ethanol productivity without fermentation inhibitors
DFT	Density functional theory method
MLR	Multiple linear regression
SPSS	Statistical product and service solutions
I	calculated inhibition values
$c_n$	regression coefficients
$D_n$	molecular descriptors
CV	Cross-validation

LOO	Leave-one-out
$Q_{LOO}^2$	Leave-one-out determination coefficient
RMSE	Root mean square error
$R^2$	Correlation coefficients
VIF	Variance inflation factor
MATLAB	Matrix laboratory
P	Significance level
F	Variance ratio
SE	Standard error of regression
IC <sub>50</sub>	Median lethal concentrations
AI	additive index methods
TU <sub>i</sub>	Inhibitory unit of component <i>i</i>
$c_i$	Concentration of component <i>i</i>
M	Inhibitory unit of a mixture
RNA	Ribonucleic Acid
MAX ( $R^2$ )	Largest correlation coefficients
MAX ( $Q^2$ )	Largest leave-one-out determination coefficient
DM	Dipole moment
TH	Total charge of hydrogen atom
LogP	Hydrophobicity
TO	Total charge of oxygen atom
qH <sup>+</sup>	Maximum positive charge of hydrogen atom
qC <sup>+</sup>	Maximum positive charge of carbon atom

constituents and concentrations of these fermentation inhibitors are influenced by the type of raw materials and the intensity of pretreatment [11]. The individual fermentation inhibition of these fermentation inhibitors were investigated extensively [10–14]. However, there was a lack of systematic study on the effects of fermentation inhibitors on bioethanol production at different concentrations. Moreover, limited information was available on the combined fermentation inhibition of the main fermentation inhibitors in pretreated hydrolysate. Therefore, it is necessary to develop data modeling tools for systematically investigating the fermentation inhibition of fermentation inhibitors that exist in pretreated lignocellulose hydrolysate.

The quantitative structure-activity relationship (QSAR) model has been used extensively for the prediction of fermentation inhibition, in which, mathematical models are constructed to reduce the experimental cost. It is a useful tool for describing the quantitative relationship between molecular structure properties and biological activity [15,16]. This is the first time that the QSAR model applied by our research team in the domain of fermentation inhibition evaluation and in the prediction of by-products that exist in lignocellulose hydrolysate [3]. In our previous study, the fermentation inhibition of lignocellulose-derived inhibitors on the growth of *Saccharomyces cerevisiae* (*S. cerevisiae*) has been evaluated successfully [17]. However, the influence of fermentation inhibitors on subsequent bioethanol production has not been investigated further.

In the present study, *S. cerevisiae* was selected as the fermentation strain for bioethanol production. Based on multiple reliable QSAR models, the individual fermentation inhibition of nineteen representative fermentation inhibitors at different concentrations on bioethanol production were investigated. Since ferulic acid was regarded as the major fermentation inhibitor in alkali-pretreated lignocellulose hydrolysate in our previous study [3,18], the combined fermentation inhibition between ferulic acid and other representative fermentation inhibitors were explored at different concentration ratios of binary mixtures. This study could provide an innovative methodology for evaluating the inhibition of inhibitors in the field of bioethanol production, thus guiding us to eliminate the strongest inhibitory by-products that existed in pretreated lignocellulose hydrolysates.

## 2. Materials and methods

### 2.1. Materials

#### 2.1.1. Chemicals

Nineteen soluble fermentation inhibitors that appeared in lignocellulose hydrolysate were selected for the fermentation inhibition test, which included phenolic compounds (ferulic acid, 4-hydroxybenzaldehyde, syringic acid, acetovanillone, vanillin, syringaldehyde, 4-hydroxyacetophenone, vanillyl alcohol, acetosyringone, sinapic acid, 4-coumaric acid, vanillic acid, 4-hydroxybenzoic acid, and salicylic acid), furan derivatives (furfural and 5-hydroxymethylfurfural (5-HMF)), weak acids (formic acid and acetic acid) and ethanol, were summarized in Tables 1a and 1b. All of the chemicals were purchased from Sinopharm Chemical Reagent Co., Ltd., China, and were of analytical purity grade. To study the individual fermentation inhibition purposefully, all fermentation inhibitors were added separately into the yeast peptone glucose liquid medium, instead of utilizing the complex lignocellulose hydrolysate as a research objective.

#### 2.1.2. Microorganism

*Saccharomyces cerevisiae*, which was obtained from China Center of Industrial Culture Collection (CICC), was used as the target microorganism for the fermentation inhibition test of fermentation inhibitors. It was cultivated in the yeast peptone glucose liquid medium (YPG, 10 g/L yeast extract, 20 g/L peptone, and 20 g/L glucose) with a shaking speed of 150 rpm at 30°C. Then, the *S. cerevisiae* was harvested by centrifuging at 4000 rpm for 5 min. The harvested cells were washed with sterile water, and clean cells in the logarithmic growth phase were collected for the subsequent fermentation inhibition test.

### 2.2. Methods

#### 2.2.1. Individual fermentation inhibition evaluation by building QSAR models

2.2.1.1. Acquisition of fermentation inhibition data (Experimental study). The batch fermentation experiment for bioethanol production was carried out in a 100 mL serum bottle containing 50 mL of YPG. Because the QSAR model of different inhibitors are needed to be established at the same concentration, the concentrations of

**Table 1a**  
The main fermentation inhibitors used in the experiment.

Number	Type	CAS Number	Name of inhibitors	Molecular structure of inhibitors
1	Phenols	1135-24-6	Ferulic acid	
2	Phenols	530-57-4	Syringic acid	
3	Phenols	123-08-0	4-Hydroxybenzaldehyde	
4	Phenols	498-02-2	Acetovanillon	
5	Phenols	121-32-4	Vanillin	
6	Phenols	134-96-3	Syringaldehyde	
7	Phenols	99-93-4	4-Hydroxyacetophenone	
8	Phenols	498-00-0	Vanillic alcohol	
9	Phenols	2478-38-8	Acetosyringone	
10	Phenols	530-59-6	Sinapic acid	
11	Phenols	7400-08-0	4-Hydroxycinnamic acid	
12	Phenols	121-34-6	Vanillic acid	

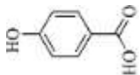
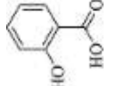

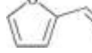


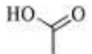
fermentation inhibitors were set at the same level. However, the solubility of these fermentation inhibitors were different. To ensure that all the fermentation inhibitors could be dissolved for exerting their maximum inhibitory effect, the suitable concentration range was chosen based on the previous research [19]. Fermentation inhibitors were added to the medium separately after sterilization at the same concentration levels of 1, 3, 5, 6, 7, 8, 9, and 11 mM. Notably, to obtain the median lethal concentration of fermentation inhibitors for the subsequent combined inhibition test, inhibitors with weak fermentation inhibition (such as formic acid, furfural and vanillic acid) were set at different levels.

The pure *S. cerevisiae*, which was grown in the logarithmic growth

phase, was prepared for cell suspension. It was cultured in the liquid medium, which was mentioned above. The concentration of *S. cerevisiae* cells was maintained at 0.8 g/L (dry weight) before fermentation, which was determined according to the OD<sub>600</sub> values by using ultraviolet–visible spectrophotometry (UV/Vis, UV-2501PC/2550, SHIMADZU, JPN) at 600 nm. The rotation rate of the batch fermentation experiment was maintained at 165 rpm with a pH of 5.48. After 8 h (logarithmic phase) of fermentation by *S. cerevisiae* at 40°C, 5 mL of fermentation broth was centrifuged at 4000 rpm for 5 min for further bioethanol analysis. The logarithmic phase was selected by the results of fermentation cycle, which was shown in the supplementary material.

The production of bioethanol was determined by using gas

**Table 1b**  
The main fermentation inhibitors in the experiment.

Number	Type	CAS Number	Name of inhibitors	Molecular structure of inhibitors
13	Phenols	99-96-7	4-Hydroxybenzoic acid	
14	Phenols	69-72-7	Salicylic acid	
15	—	64-17-5	Ethanol	
16	Furans	98-01-1	Furfural	
17	Furans	67-47-0	5-Hydroxymethylfurfural	
18	Fatty Acids	64-18-6	Formic acid	
19	Fatty Acids	64-19-7	Acetic acid	

chromatography (GC, Agilent 7890 A, USA) with the flame ionization detector. GC was performed with an HP-INNOWax capillary column (60 m × 320 μm × 0.5 μm) equipped with an automatic headspace sampler (HS<sup>9</sup> A, China). Helium was used as a carrier gas, and the flow rate was 2 mL/min (180°C). The operation conditions of the automatic headspace sampler were as follows: VIAL (headspace vial temperature) = 70°C; LOOP (coil temperature) = 80°C; TR. LINE (conveyor belt temperature) = 90°C; vial pressurization time = 0.2 min; loop fill time = 1 min; and VIAL EQ.TIME (headspace vial equilibration time) = 10 min. The volume of the sample loop was 1 mL. Triplicate experiments were performed in the study.

It is worth noting that the fermentation inhibition values were expressed by the reduction rate of ethanol productivity, which could be calculated as follows:

$$\text{Inhibition}(\%) = \frac{Q_C - Q}{Q_C} \times 100\% \quad (1)$$

where Q and Q<sub>C</sub> are the ethanol productivity (g/L at 8 h) that was influenced by inhibitors and was not influenced by inhibitors, respectively.

**2.2.1.2. Calculation of molecular descriptors.** To convert the molecular structure properties of fermentation inhibitors into quantified variables, the molecular descriptors were calculated by using GAUSSIAN 2009 and CHEMBIOOFFICE 2012 software. The 24 frequently used molecular descriptors, which were selected by referring to the previous studies, were calculated by using the density functional theory method (DFT) that based on the optimized molecular structures of all of the fermentation inhibitors [20]. The molecular descriptors included electrostatic properties, orbit properties, polarity/dipole/volume/space properties and thermodynamic properties [3] in which the electrophilic index could be calculated by Eq. (2). It is worth noting that the physicochemical properties (hydrophobic constant (logP) and ionization constant (pKa)) were ascertained based on CHEMBIOOFFICE 2012 software. The energy of the whole molecular structure was minimized to the B3LYP/6-31G\*\* level by using GAUSSIAN 2009 software [21]. Meanwhile, no imaginary frequencies were discovered in the optimal structure. All the molecular descriptors that used in the study were summarized in the supplementary materials.

$$\omega = \frac{E_{\text{HOMO}}^2 + 2E_{\text{HOMO}}E_{\text{LUMO}} + E_{\text{LUMO}}^2}{4(E_{\text{LUMO}} - E_{\text{HOMO}})} \quad (2)$$

where E<sub>HOMO</sub> and E<sub>LUMO</sub> represent the highest occupied molecular orbital and the lowest unoccupied molecular orbital, respectively.

**2.2.1.3. Establishment and validation of QSAR models (Model establishment).** The multiple linear regression (MLR) method was introduced to establish QSAR models. The MLR equations are presented by Eq. (3). The most appropriate variables were selected from the 24 frequently used molecular descriptors by the stepwise elimination of independent variables by using statistical product and service solutions (SPSS) software [22,23]. The inhibition values and calculated molecular descriptors were used as dependent variables and independent variables, respectively.

$$I = c_0 + c_1D_1 + c_2D_2 + c_3D_3 + \dots + c_nD_n \quad (3)$$

where  $c_0, c_1, c_2, c_3, \dots,$  and  $c_n$  are used to describe the regression coefficients;  $D_1, D_2, D_3, \dots,$  and  $D_n$  are used to describe the molecular descriptors; and I represents the calculated inhibition values.

The established QSAR models were validated by using cross-validation (CV) through the leave-one-out (LOO) procedure to confirm their preferable prediction performance and practicability. The LOO determination coefficient (Q<sub>LOO</sub><sup>2</sup>) and the root mean square error (RMSE) were obtained as statistical parameters [22]. Y-scrambling validation was applied to check the predictability and stability of QSAR models further. The correlation coefficients (R<sup>2</sup>) and LOO determination coefficients (Q<sub>LOO</sub><sup>2</sup>) were obtained from 100 randomly generated QSAR models, which should be lower than that of the original models [21]. Besides, to avoid the over-fitting phenomena, the ratios of the modelling variables to the sample size should be greater than 1:5. Meanwhile, the collinearity among the modelling variables needed to be reduced by evaluating the variance inflation factor (VIF) [24]. All validations were executed by using MATLAB software. Moreover, the regression equations needed to meet the requirements, which were assessed by the fitting parameters, including the significance level (P), correlation coefficient (r<sup>2</sup>), variance ratio (F), standard error of regression (SE) [3]. It should be pointed out that all of the established QSAR models for individual inhibition evaluation were developed based on the inhibition data at the different concentrations of inhibitors.

## 2.2.2. Combined fermentation inhibition evaluation by building QSAR models

**2.2.2.1. Acquisition of the fermentation inhibition data (IC<sub>50</sub>) (Experimental study).** Concentration-response curves were established by using the data from individual fermentation inhibition tests. The median lethal concentrations (IC<sub>50</sub>, the concentration of 50% inhibition on bioethanol yield) and the corresponding 95% confidence interval were obtained from concentration-response curves by using OriginPro

9.1 software [25]. The unit of the IC<sub>50</sub> values was denoted as mM for investigative lignocellulose-derived inhibitors.

According to our previous study, ferulic acid possessed a stronger inhibition value and a higher concentration in alkali-pretreated lignocellulose hydrolysate [3,18]. Therefore, it was selected as the objective for the evaluation of the combined fermentation inhibition of the main lignocellulose-derived inhibitors on bioethanol production. Then, it was mixed in pairs with the other representative soluble fermentation inhibitors according to previous inhibition experiments [3,26], which included phenolic compounds (vanillin, syringaldehyde, vanillic acid, and 4-hydroxybenzaldehyde), furan derivatives (furfural) and weak acids (formic acid). To observe the effect of different mixed concentrations on the combined fermentation inhibition, different ferulic acid concentrations were set in the experiment, including low, medium and high levels (20%, 50%, and 80% × IC<sub>50</sub>) [27]. The combined fermentation inhibition of each mixture were determined by following the procedure of the single fermentation inhibition evaluation.

2.2.2.2. Evaluation methods for combined fermentation inhibition (Model establishment). The types of combined fermentation inhibition on the binary mixtures were evaluated by the additive index (AI) methods. The inhibitory unit (TU) was calculated by the following equation [28].

$$TU_i = \frac{c_i}{LC_{50,i}} \quad (4)$$

where  $TU_i$  is the inhibitory unit of component  $i$  in the binary mixtures;  $c_i$  is the concentration of component  $i$  when the mixtures produced 50% inhibition on bioethanol yield; and  $LC_{50,i}$  is the median lethal

concentration of the component  $i$  action alone.

The inhibitory unit of a mixture ( $M$ ) corresponds to the sum of  $TU_i$ . Then, AI could be calculated by following Eqs. (5) and (6). The types of combined fermentation inhibition of binary mixtures were determined as follows:  $M = 1$  or  $AI = 0$  (simple additive effect);  $M < 1$  or  $AI > 0$  (synergistic effect);  $M > 1$  or  $AI < 0$  (antagonistic effect) [27].

$$AI = 1/M - 1.0 (M \leq 1) \quad (5)$$

$$AI = 1.0 - M (M > 1) \quad (6)$$

It should be noted that a simple additive effect was considered to be  $M = 1$  or  $AI = 0$  in an ideal situation [29]. However, the simple additive effect in the actual situation was re-defined as  $M$  (from 0.870 to 1.230) and  $AI$  (from -0.233 to 0.149), following the report by Broderius et al. (1995) [30].

### 3. Results and discussion

#### 3.1. Effect of lignocellulose-derived inhibitors on bioethanol production

Nineteen fermentation inhibitors, which existed in the pretreated lignocellulose hydrolysate, were preliminarily investigated for their fermentation inhibition on bioethanol production by concentration-response curves at different concentrations (shown in Fig. 1). The bioethanol yield decreased significantly after adding most of the above fermentation inhibitors, which showed that the presence of fermentation inhibitors in lignocellulose hydrolysate did have a negative effect on the fermentation process at a specific concentration range. However, part of the fermentation inhibitors (such as vanillic alcohol and

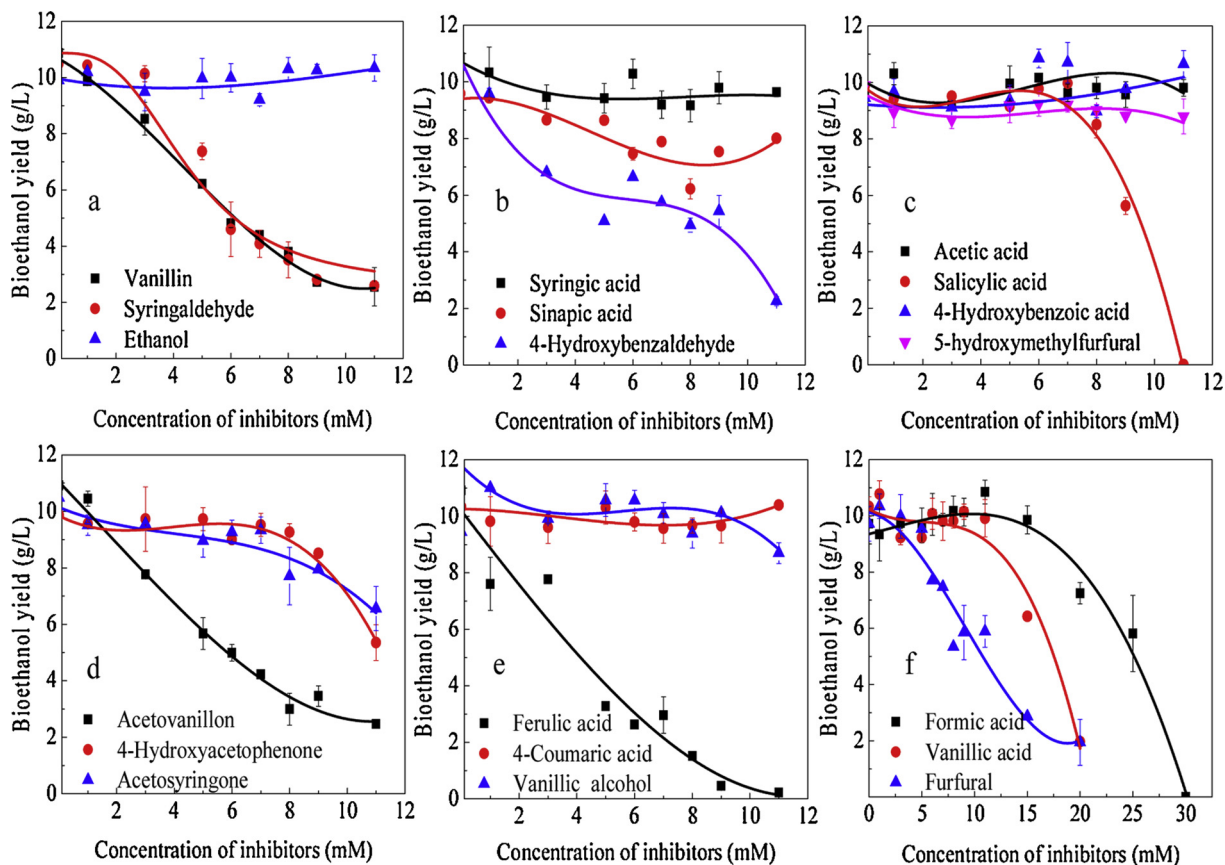


Fig. 1. The influence of the representative fermentation inhibitors on bioethanol production at different concentrations. Error bars are used to reflect the standard deviations, which might be covered with symbols in some cases. a) vanillin, syringaldehyde and ethanol; b) syringic acid, sinapic acid and 4-hydroxybenzaldehyde; c) acetic acid, salicylic acid, 4-hydroxybenzoic acid and 5-hydroxymethylfurfural; d) acetovanillon, 4-hydroxyacetophenone and acetosyringone; e) ferulic acid, 4-coumaric acid and vanillic alcohol; f) formic acid, vanillic acid and furfural.

ethanol) could increase bioethanol production at certain concentrations, which was attributed to the hormesis effect [31]. Hormesis effect was defined as different roles which were played by inhibitors on microorganisms at different concentrations. The inhibitors contributed stimulatory effect on microorganisms at lower inhibitory concentration because of the micro-interference towards cell homeostasis, while they might play an inhibitory effect at higher inhibitory concentrations.

It was found that phenolic compounds exhibited stronger fermentation inhibition on bioethanol production than that of furan derivatives and weak acids. As an important phenolic compound, ferulic acid exhibited the strongest fermentation inhibition of the fermentation inhibitors at the same concentration. Meanwhile, the fermentation inhibition of furfural were stronger than that of 5-HMF, and the result was consistent with our previous studies [3,18].

It was reported that phenolic inhibitors had fermentation inhibition on the fermentation process by producing intracellular reactive oxygen species, which could hinder the synthesis of RNA and protein [32,33]. Furan inhibitors (including mainly furfural and 5-HMF) could inhibit the activities of alcohol dehydrogenase, pyruvate dehydrogenase and aldehyde dehydrogenase in microorganisms, thus decelerating the growth rate of *S. cerevisiae* [12,34]. It also was reported that weak acids could inhibit the growth of *S. cerevisiae* by acidizing the intracellular environment [34]. However, none of the above studies revealed the relationship between the fermentation inhibition and the molecular structure of lignocellulose-derived inhibitors.

In our present research, we found that the fermentation inhibition had a strong correlation with the molecular structure of fermentation inhibitors. For instance, ferulic acid showed a stronger fermentation inhibition on bioethanol production, which might have originated from the positive interactions between unsaturated bonds and carboxyl groups. It was worth noting that electron activity differences were showed among different atoms of double bonds. Therefore, the greater nucleophilic reaction between fermentation inhibitors and the protein of *S. cerevisiae* could be easily occurred due to the presence of permanent polarization [35]. Furfural exhibited a stronger fermentation inhibition than that of 5-HMF, which might have been due to the higher number of electronegative oxygen atoms in its molecule that can easily generate a hydrogen bond, thus increasing the interaction between fermentation inhibitors and intracellular bio macromolecules. Additionally, the hydrogen production was intensely inhibited by furfural compared to 5-HMF, which could give rise to less reducing power for the conversion from R-CHO to RCH<sub>2</sub>OH [36]. The above results would provide a theoretical basis for establishing the following QSAR models.

### 3.2. Individual fermentation inhibition evaluation by QSAR models

#### 3.2.1. Establishment and validation of QSAR models

To evaluate the fermentation inhibition precisely and to analyze the inhibition mechanisms of individual fermentation inhibitors systematically, QSAR models were established at different fermentation inhibitor concentrations. Due to the inhibition rates of lignocellulose-derived fermentation, the inhibitors were not significant at low concentrations (1, 3, and 5 mM), and the QSAR models were established at different concentrations of 6, 7, 8, 9, and 11 mM. The inhibition rates of various fermentation inhibitors on the bioethanol yield and their different molecular descriptors were used to build QSAR models by the MLR method. The established QSAR models were validated by the statistical parameters, which included model validation coefficients and fitting parameters. All of the parameters were obtained from LOO cross validation, Y-scrambling validation and regression equations (shown in Table 2).

It was found that the predictability, stability and fitting ability of all the established QSAR models were satisfied with demands. The differences between r<sup>2</sup> and Q<sup>2</sup><sub>LOO</sub> were less than 0.3, and all of them were larger than 0.5. P values, which were obtained from the significance test, were smaller than 0.05. The result indicated that the error caused

**Table 2**  
QSAR models and statistical parameters for individual fermentation inhibition of fermentation inhibitors.

Model number	Inhibitor concentrations (mM)	QSAR models	Fitting parameters			Validation parameters					
			r <sup>2</sup>	F	P	VIF	MAX(R <sup>2</sup> )	MAX(Q <sup>2</sup> )	Q <sup>2</sup> <sub>LOO</sub>	RMSE	SE
A	6	I = -0.179 + 0.085 × DM - 0.663 × TH + 0.229 × LogP - 0.064 × TO	0.888	21.744	0.000	(1.493;3.308;3.328;3.947)	0.352	0.214	0.801	0.077	0.103
B	7	I = -0.117 + 0.081 × DM - 0.735 × TH + 0.247 × LogP - 0.070 × TO	0.845	14.976	0.000	(1.493;3.308;2.328;3.947)	0.245	-0.048	0.713	0.095	0.126
C	8	I = -0.207 + 0.108 × DM - 0.647 × TH + 0.243 × LogP - 0.066 × TO	0.863	17.660	0.000	(1.493;3.308;2.328;3.947)	0.650	0.582	0.724	0.099	0.142
D	9	I = -0.187 + 0.101 × DM - 0.778 × TH + 0.253 × LogP + 0.765 × qH <sup>+</sup>	0.879	19.941	0.000	(1.583;3.302;3.751;6.325)	0.380	0.025	0.724	0.099	0.148
E	11	I = -0.122 + 0.104 × DM - 0.965 × TH + 0.467 × LogP + 0.097 × qC <sup>+</sup>	0.860	16.860	0.000	(1.583;3.302;3.751;6.325)	0.349	0.387	0.627	0.124	0.199

Notes: QSAR models were established with fermentation inhibitors at different concentrations of 6, 7, 8, 9, and 11 mM, respectively. I indicated the individual inhibition effects of the fermentation inhibitors, which had the linear correlation with the different molecular descriptors at the different concentrations of inhibitors, including DM (the dipole moment), TH (the total charge of hydrogen atom), LogP (the hydrophobicity), TO (the total charge of oxygen atom), qH<sup>+</sup> (the maximum positive charge of hydrogen atom) and qC<sup>+</sup> (the maximum positive charge of carbon atom), respectively. These molecular descriptors were used to describe the physico-chemical or electrostatic characteristics. Fitting parameters were used to describe the fitting ability of QSAR models, including r<sup>2</sup> (the correlation coefficient), F (the variance ratio), P (the significance level), and VIF (the variance inflation factor), respectively. Validation parameters were adopted to describe the predicted ability of QSAR models, including MAX(R<sup>2</sup>) (maximum R<sup>2</sup>, obtained from the randomly generated models), MAX(Q<sup>2</sup>) (maximum Q<sup>2</sup>, obtained from the randomly generated models), Q<sup>2</sup><sub>LOO</sub> (the LOO determination coefficients), RMSE (the root mean square error) and SE (the standard error of regression), respectively.

by accidental factors was minimal. The SE and RMSE of all of the established QSAR models were relatively small. Meanwhile, the F values were relatively greater in certain degrees of freedom. The values of MAX ( $R^2$ ) and MAX ( $Q^2$ ), which were acquired from the randomly generated 100 models by Y-scrambling validation, were smaller than the  $r^2$  and  $Q_{LOO}^2$  values of the original models. It was indicated that the established QSAR models were stable and had less relevant contingency. Moreover, the VIF values were smaller than 10, which represented weak collinearities among the independent variables, while the established models were stable and acceptable.

To validate the predicted performance of established QSAR models, the predicted values were compared with the experimental values at different concentrations (shown in Fig. 2). The predicted values were calculated by LOO cross validation and MLR equations, which are expressed as the black points and red points, respectively. The black diagonal lines are used to evaluate the perfect unity between the predicted values and the experimental values. The predicted toxicity values were evenly distributed near the black diagonal lines, which indicates that the predictability of the established QSAR models was perfect [21,22].

### 3.2.2. Fermentation inhibition evaluation by QSAR models and mechanism study

Based on the established QSAR models, the inhibition values of various kinds of fermentation inhibitors were calculated to predict their fermentation inhibition on bioethanol production to minimize the

experimental cost (shown in Fig. 3). It was found that the fermentation inhibition of phenolic aldehyde was stronger than that of phenolic acid followed by phenolic alcohol, which was influenced by the position of the functional group on the benzene ring. Phenolic aldehyde was more prone to occur the nucleophilic addition reaction with carbonyl group in the presence of ammonia, which could also be transformed into a reactive nucleophile which could work on the intracellular bio macromolecules, thus expressing its strongest fermentation inhibition [37]. Meanwhile, the fermentation inhibition of aromatic acids were stronger than that of fatty acids. Among them, the inhibition values of vanillin (53.014%, 56.913%, 68.815%, 77.906%, and 72.288%) were less than that of cinnamaldehyde (69.2878%, 75.6812%, 83.4572%, and 76.8556%). The result might be due to the presence of the electron-donating methoxy group, which weakened the fermentation inhibition by passivating the benzene ring in inhibitor molecules. It was found that the electron-donating methoxy group could cause relative lower electron deficiency, thus reducing the probability of fermentation inhibitors that was reacted with bio nucleophiles [35]. Furthermore, the low molecular weight of the cinnamic acid facilitated its entry into *S. cerevisiae* cells to react with internal substances<sup>31</sup>. The same result could be obtained from the inhibition values comparison between vanillic acid (7.182%, 11.31%, 13.791%, 9.401%, and 17.305%) and syringic acid (7.962%, 11.484%, 16.523%, 2.374%, and 4.416%). It was found that the inhibition values of 4-coumaric acid (2.688%, 4.095%, 14.263%, 18.135%, and 7.785%) were less than that of cinnamic acid (25.6213%, 29.8865%, 35.998%, 68.1463%, and 41.947%),

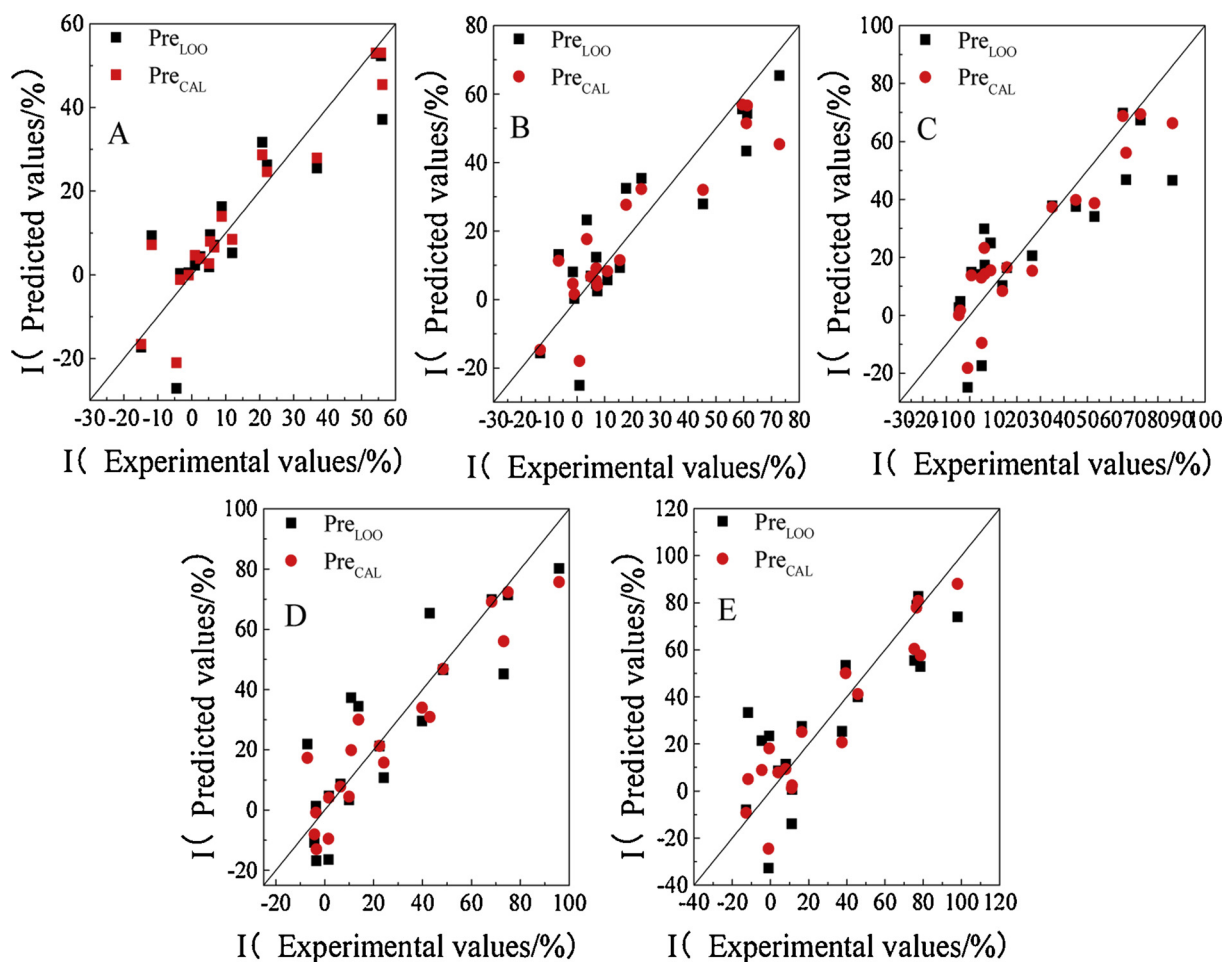


Fig. 2. Experimental values versus predicted values of fermentation inhibitors at different concentrations.

QSAR models at different concentrations (6, 7, 8, 9, and 11 mM) are expressed as A, B, C, D, and E, respectively. Pre<sub>CAL</sub> is used to describe the predicted inhibition values of fermentation inhibitors, which was calculated by QSAR models. Pre<sub>LOO</sub> is used to describe the predicted inhibition values of fermentation inhibitors, which was calculated by LOO cross validation.

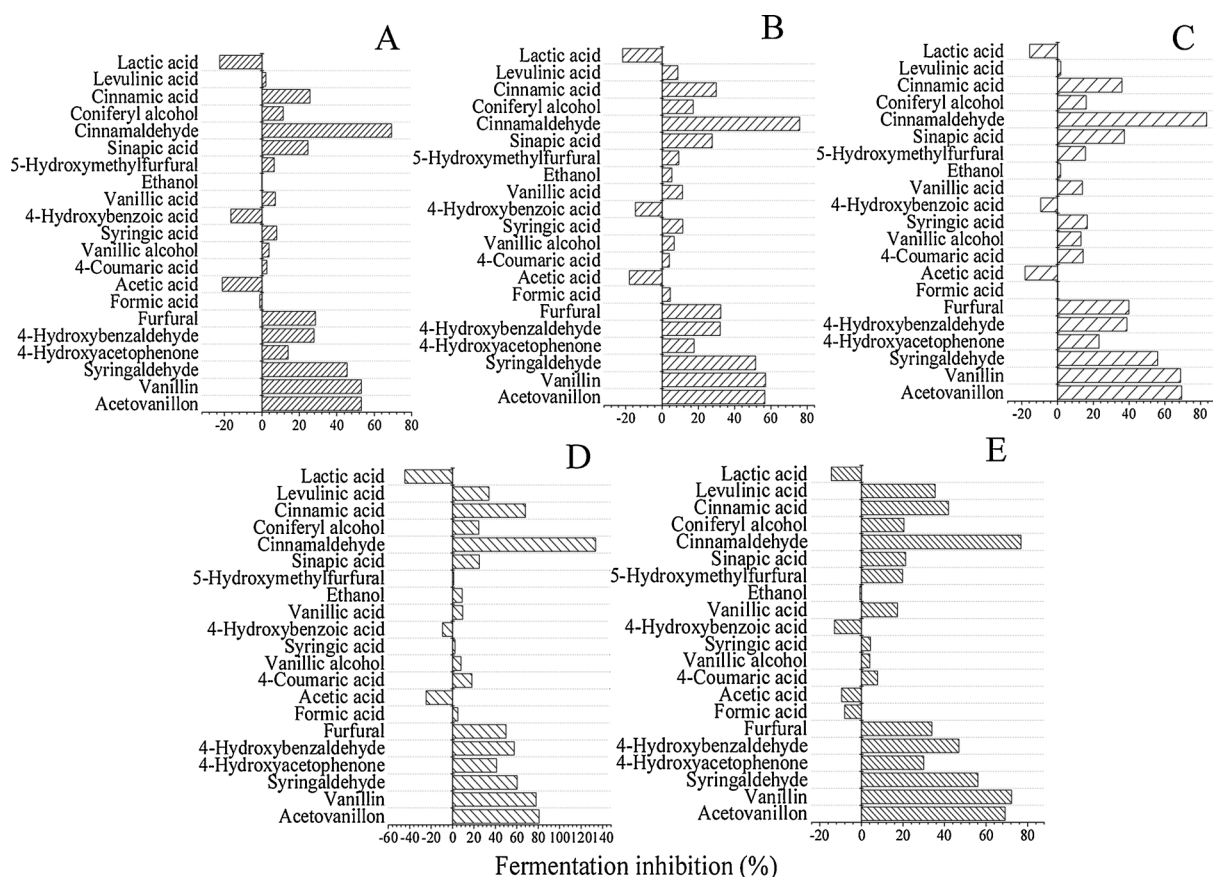


Fig. 3. Individual fermentation inhibition prediction of lignocellulose-derived inhibitors by using QSAR models.

A, B, C, D and E are used to express different individual fermentation inhibition predictions at 6, 7, 8, 9, and 11 mM, respectively.

which might be due to the presence of intramolecular hydrogen bonds of fermentation inhibitors could reduce the interaction of hydrogen bonds on bio macromolecule. These above results were consistent with the studies of Klinke et al. (2004) and Gu et al. (2014) [38,39].

The data in Table 2 reversed the strong relationship between the structural properties of molecules (expressed by molecular descriptors) and the fermentation inhibition of fermentation inhibitors. Fermentation inhibitors played a role in inhibiting bioethanol production by influencing the following two processes, which were the diffusion of inhibitors into the microbial cells and the reaction with other substances in *S. cerevisiae* [3]. DM, TH, and log P could be used to describe the diffusion process, while TO,  $qH^+$ , and  $qC^+$  are used to express the reaction step in which DM is the total dipole moment of the fermentation inhibitors molecule, which has a positive correlation with the inhibition values because of the existence of C=O. Due to the dissimilarity of the electronegativity between different atoms in the C=O functional group, permanent polarization was presented. The polarized C atom plays an important role in dominating the fermentation inhibition of fermentation inhibitors by forming a bond with the target site (such as protein) in the microbial cells [35]. LogP describes the possibility of fermentation inhibitors entering the microbial cells. It has an impact on the fermentation inhibition of fermentation inhibitors, which would be influenced by the diffusion of fermentation inhibitors from the fermentation broth to microbial cells before inhibition occurred, thus controlling the number of fermentation inhibitors which were interacted with microbial cells [40]. TH is the total charge of the H atom in the fermentation inhibitor molecule, which represents the charge distribution of investigative inhibitors. It was assigned to electrostatic properties that defined the electrophilic reactivity with intracellular substances [3,35]. Furthermore, TO describes the total net charge of the O atom in the fermentation inhibitor molecule, which is

necessary to reflect the electronic reactivity by charge distribution that dominated the interaction between fermentation inhibitors and microbial cells [35].  $qC^+$  and  $qH^+$  were the maximum positive charge of the carbon atom and the hydrogen atom, respectively, which indicated the molecular stability and hydrogen bond-forming ability.  $qC^+$  had a positive correlation with fermentation inhibition, which might be because the stable fermentation inhibitors increased the probability of effective fermentation inhibitors reacting with intracellular bio macromolecule. Additionally,  $qH^+$  also played a positive role in dominating the fermentation inhibition due to the increased hydrogen bond-forming ability between fermentation inhibitors and intracellular bio macromolecule.

It is noting worth that DM, TH, and logP were all included in the five established QSAR models, which indicated that diffusion of inhibitors from the solution to yeast cells (expressed by logP) and their affinity (expressed by DM and TH) to yeast cells were the primary and necessary process for generating fermentation inhibition by fermentation inhibitors. However, TO,  $qH^+$ , and  $qC^+$  appeared dispersed in the five QSAR models. Furthermore, it was found that the fermentation inhibition of the fermentation inhibitors were highly related to TO at low concentrations (models A, B, and C), whereas they were highly relative with  $qC^+$  and  $qH^+$  at high concentrations (models D and E). The appearance of TO in models A, B, and C illustrates that the electric charge distribution of the O atom dominated the reaction step of fermentation inhibitors at low concentrations, whereas the appearance of  $qC^+$  and  $qH^+$  in models D and E manifests the importance of molecular stability and the hydrogen bond-forming ability in the reaction step of fermentation inhibitors at high concentrations.



### 3.3. Combined fermentation inhibition evaluation of representative fermentation inhibitors on bioethanol production

Fermentation inhibitors, which were co-existed in lignocellulose hydrolysates, usually exhibited a combined fermentation inhibition by the interactions among them. Many previous studies investigated the combined fermentation inhibition of binary mixtures in lignocellulose hydrolysate at different concentrations. The results showed that furan derivatives, which were obtained from the pentose degradation, exhibited synergistic effect when acting with weak acids (formic acid, acetic acid, and levulinic acid). However, the combined fermentation inhibition when acting with the other binary mixtures were roughly simple additive effect [12,13]. Considering the complexity of lignocellulose hydrolysate in terms of the type and amount of fermentation inhibitors, and less studies were focused on the combined fermentation inhibition effect of actual alkali pretreated hydrolysates, the representative fermentation inhibitors of ferulic acid and the other phenols, furans and weak acids were selected to investigate their combined fermentation inhibition based on the previous study [3,27].

The combined fermentation inhibition between ferulic acid and the other representative fermentation inhibitors are shown in Table 3. The mixture ratio of ferulic acid at 50% × IC<sub>50</sub> between all fermentation inhibitors, antagonism and the simple additive effect existed simultaneously by evaluating the M values and AI values, the values of which ranged from 1.023 to 1.789 and -0.789 to -0.023, respectively. Three kinds of binary mixtures, which included ferulic acid and syringaldehyde, ferulic acid and furfural, and ferulic acid and formic acid, were the simple additive effect accompanied by M values from 1.023 to 1.282 and AI values from -0.282 to -0.023. It is worth noting that the combined fermentation inhibition for the binary mixture of ferulic acid and syringaldehyde belonged to the weak simple additive effect due to the close proximity of the obtained M values (1.282) and the AI values (-0.282) to the given ranges. With the mixture ratio of ferulic acid at 20% × IC<sub>50</sub> between fermentation inhibitors, most of the combined fermentation inhibition exhibited a simple additive effect, which was determined by the M values (ranging from 0.892 to 1.726) and the AI values (ranging from -0.726 to 0.121). However, the binary mixture between ferulic acid and vanillic acid was antagonism. With the mixture ratio of ferulic acid at 80% × IC<sub>50</sub> between fermentation inhibitors, the combined fermentation inhibition for most binary mixtures belonged to antagonism based on the evaluation of the M values (varying from 1.175 to 2.343) and the AI values (varying from -1.343 to -0.175). It was indicated that the simple additive effect was found mainly in the binary mixture when the concentration of ferulic acid was

low. However, antagonism occurred when the concentration of ferulic acid was high. This phenomenon verified the important role of the combined inhibition of ferulic acid in the binary mixtures. These above results confirmed that the combined fermentation inhibition of binary mixtures except furan derivatives was roughly simple additive effect, which were consistent with the previous studies [12,13]. However, synergistic effect was not appeared when furfural and ferulic acid were mixed together, which was different with the previous research. This might because the relatively low inoculation of *S. cerevisiae* was used in this study [12].

According to the results of the established QSAR models of the individual fermentation inhibition, the combined fermentation inhibition were speculated to be hydrophobic effects, hydrogen bonds and electrostatic interactions among inhibitors. For instance, some hydrophobic inhibitors might generate the hydrophobic interactions among different fermentation inhibitors. Some fermentation inhibitors, which contained a specific functional group (such as -COOH, -OH groups), would form hydrogen bonds among different inhibitors. Furthermore, electrostatic attraction between phenolic and carboxylic groups of fermentation inhibitors could be formed when the binary fermentation inhibitor mixtures possessed opposite electrical charges [41]. The above inhibition mechanisms would lead to a decrease in the number of effective fermentation inhibitors that act on *S. cerevisiae* cells at high ferulic acid concentrations; therefore, the total fermentation inhibition of the inhibitors were weakened (expressed as the antagonism effect). It should be pointed out that although *S. cerevisiae* was chosen as the representative yeast for bioethanol production in this work, the methodology that was used in the present study could provide us with an innovative way to investigate the individual and combined fermentation inhibition of inhibitors on bioethanol production by other types of yeasts.

Considering the strong fermentation inhibition of ferulic acid, it should be removed in priority. Actually, we have already built a new powerful detoxification system successfully which could alleviate ferulic acid in situ according to the result of this research [18]. Meanwhile, the inhibition effects of the other representative fermentation inhibitors (such as furfural and vanillin) should be also removed based on the obtained inhibition mechanisms. The mechanism study showed that the formation of hydrogen bonding among fermentation inhibitors could reduce the number of fermentation inhibitors which were interacted with biological macromolecules. Thus, new absorbent could be applied to alleviate the inhibition effects of fermentation inhibitors, which will be studied in our near future work. In addition, the reduction of fermentation inhibitors and favorable fermentation process

**Table 3**  
Joint fermentation inhibition evaluation of the main fermentation inhibitors in lignocellulose hydrolysate.

Mixture	Dose effect curve	R <sup>2</sup>	Mixture ratios of ferulic acid (× IC <sub>50</sub> )	IC <sub>50</sub> and 95% confidence interval	M	AI	Types of joint toxicity effects
Ferulic acid + vanillin	Hill1	0.920	20%	6.831[3.899, 11.846]	1.246	-0.246	Weak simple addition
	Logistic	0.992	50%	6.534[5.745, 7.417]	1.335	-0.335	Antagonism
	DoseResp	0.962	80%	6.569[4.880, 9.223]	1.526	-0.526	Antagonism
Ferulic acid + syringaldehyde	Hill1	0.995	20%	5.603[4.915, 6.306]	0.907	0.102	Simple addition
	Slogistic1	0.987	50%	6.828[6.325, 7.575]	1.282	-0.282	Weak simple addition
	Hill1	0.982	80%	5.263[4.237, 6.443]	1.175	-0.175	Simple addition
Ferulic acid + vanillic acid	DoseResp	0.998	20%	24.815[18.731, 30.877]	1.726	-0.726	Antagonism
	DoseResp	0.997	50%	13.708[13.002, 14.729]	1.311	-0.311	Antagonism
	DoseResp	0.999	80%	9.911[9.578, 10.375]	1.518	-0.518	Antagonism
Ferulic acid + 4-hydroxybenzaldehyde	Logistic	0.987	20%	6.403[4.565, 9.446]	0.892	0.121	Simple addition
	DoseResp	0.975	50%	10.648[9.457, 11.356]	1.789	-0.789	Antagonism
	DoseResp	0.999	80%	11.076[10.840, 11.306]	2.342	-1.342	Antagonism
Ferulic acid + formic acid	Logistic	0.997	20%	25.342[24.887, 25.585]	1.193	-0.193	Simple addition
	DoseResp	0.970	50%	15.091[14.438, 16.044]	1.023	-0.023	Simple addition
	DoseResp	0.999	80%	12.272[11.865, 12.832]	1.480	-0.480	Antagonism
Ferulic acid + furfural	Hill1	0.997	20%	11.224[10.274, 12.275]	1.105	-0.105	Simple addition
	Logistic	0.996	50%	8.764[8.105, 9.543]	1.121	-0.121	Simple addition
	Logistic	0.996	80%	7.334[6.796, 7.977]	1.340	-0.340	Antagonism

could be realized by optimizing pretreatment conditions, regulating fermentation conditions and screening the resistant fermentation strains, etc.

#### 4. Conclusion

QSAR models were successfully established to quantitatively evaluate the individual fermentation inhibition of representative fermentation inhibitors on bioethanol production in the pretreated lignocellulose hydrolysate. A strong relationship between the molecular descriptors and the fermentation inhibition of inhibitors was found. DM, TH, logP, and TO exhibited their importance at low concentrations of inhibitors, while  $qC^+$  and  $qH^+$  played an important role at high concentrations of inhibitors. The established QSAR models would be beneficial not only in predicting the individual fermentation inhibition to minimize the experimental cost but also in providing a theoretical direction for the mechanism study to reduce the fermentation inhibition by changing the physicochemical properties of fermentation inhibitors. Meanwhile, ferulic acid, which possessed a greater fermentation inhibition and a higher concentration as confirmed in our previous study in alkali-pretreated lignocellulose hydrolysate, was in charge of the types of combined fermentation inhibition for the binary mixtures in the lignocellulose hydrolysates in the present study.

#### Acknowledgments

This project is funded by National Key Research and Development Program of China (2018YFC1901005), Shanghai Committee of Science and Technology (No. 17295810603, 17DZ1202804, 18295810400) Institute of Eco-Chongming (ECNU-IEC-201901) and Shanghai Pujiang Program (17PJ1402400). The authors would like to thank them for funding this work.

#### Appendix A. Supplementary data

Supplementary material related to this article can be found, in the online version, at doi:<https://doi.org/10.1016/j.bej.2019.04.013>.

#### References

- A.M. Lopez-Hidalgo, A. Sánchez, A. De León-Rodríguez, Simultaneous production of bioethanol and biohydrogen by *Escherichia coli* WDH1 using wheat straw hydrolysate as substrate, *Fuel* 188 (2017) 19–27.
- C. Kundu, L.T.P. Trinh, H.-J. Lee, J.-W. Lee, Bioethanol production from oxalic acid-pretreated biomass and hemicellulose-rich hydrolysates via a combined detoxification process, *Fuel* 161 (2015) 129–136.
- J. Hou, C. Ding, Z. Qiu, Q. Zhang, W.-N. Xiang, Inhibition efficiency evaluation of lignocellulose-derived compounds for bioethanol production, *J. Clean. Prod.* 165 (2017) 1107–1114.
- J.-Q. Zhu, X. Li, L. Qin, W.-C. Li, H.-Z. Li, B.-Z. Li, Y.-J. Yuan, In situ detoxification of dry dilute acid pretreated corn stover by co-culture of xylose-utilizing and inhibitor-tolerant *Saccharomyces cerevisiae* increases ethanol production, *Bioresour. Technol.* 218 (2016) 380–387.
- C. Sambusiti, F. Monlau, N. Antoniou, A. Zabanitout, A. Barakat, Simultaneous detoxification and bioethanol fermentation of furans-rich synthetic hydrolysate by digestate-based pyrochar, *J. Environ. Manage.* 183 (2016) 1026–1031.
- J. Hou, S. Zhang, Z. Qiu, H. Han, Q. Zhang, Stimulatory effect and adsorption behavior of rhamnolipids on lignocellulose degradation system, *Bioresour. Technol.* 224 (2017) 465–472.
- V.P. Soudham, T. Brandberg, J.P. Mikkola, C. Larsson, Detoxification of acid pretreated spruce hydrolysates with ferrous sulfate and hydrogen peroxide improves enzymatic hydrolysis and fermentation, *Bioresour. Technol.* 166 (2014) 559–565.
- L.J. Jonsson, C. Martin, Pretreatment of lignocellulose: formation of inhibitory by-products and strategies for minimizing their effects, *Bioresour. Technol.* 199 (2016) 103–112.
- T. Saravanakumar, H.-S. Park, A.-Y. Mo, M.-S. Choi, D.-H. Kim, S.-M. Park, Detoxification of furanic and phenolic lignocellulose derived inhibitors of yeast using laccase immobilized on bacterial cellulosic nanofibers, *J. Mol. Catal., B Enzym.* 134 (2016) 196–205.
- M.A. Franden, H.M. Pilath, A. Mohagheghi, P.T. Pienkos, M. Zhang, Inhibition of growth of *Zymomonas mobilis* by model compounds found in lignocellulosic hydrolysates, *Biotechnol. Biofuels* 6 (2013) 99.
- C. Bellido, S. Bolado, M. Coca, S. Lucas, G. Gonzalez-Benito, M.T. Garcia-Cubero, Effect of inhibitors formed during wheat straw pretreatment on ethanol fermentation by *Pichia stipitis*, *Bioresour. Technol.* 102 (2011) 10868–10874.
- J. Zaldivar, A. Martinez, L.O. Ingram, Effect of alcohol compounds found in Hemicellulose Hydrolysate on the growth and fermentation of ethanogenic *Escherichia coli*, *Biotechnol. Bioeng.* 68 (2000) 524–530.
- J. Zaldivar, A. Martinez, L.O. Ingram, Effect of selected aldehydes on the growth and fermentation of ethanogenic *Escherichia coli*, *Biotechnol. Bioeng.* 65 (1999) 24–33.
- D. Cao, M. Tu, R. Xie, J. Li, Y. Wu, S. Adhikari, Inhibitory activity of carbonyl compounds on alcoholic fermentation by *Saccharomyces cerevisiae*, *J. Agric. Food Chem.* 62 (2014) 918–926.
- L. Jia, Z. Shen, W. Guo, Y. Zhang, H. Zhu, W. Ji, M. Fan, QSAR models for oxidative degradation of organic pollutants in the Fenton process, *J. Taiwan Inst. Chem. Eng.* 46 (2015) 140–147.
- M.C. Sharma, QSAR studies of novel 1-(4-methoxyphenethyl)-1H-benzimidazole-5-carboxylic acid derivatives and their precursors as antileukaemic agents, *J. Taibah Univ. Sci.* 10 (2016) 122–130.
- J. Hou, Z. Qiu, H. Han, Q. Zhang, Toxicity evaluation of lignocellulose-derived phenolic inhibitors on *Saccharomyces cerevisiae* growth by using the QSTR method, *Chemosphere* 201 (2018) 286–293.
- Q. Zhang, H. Huang, H. Han, Z. Qiu, V. Achal, Stimulatory effect of in-situ detoxification on bioethanol production by rice straw, *Energy* 135 (2017) 32–39.
- H. Han, H. Huang, Z. Qiu, Q. Zhang, Stimulatory effect of ferulic acid degrading bacteria on lignocellulose hydrolysis, *Environ. Sci. Technol.* 40 (S2) (2019) 1–5 (Chinese literature).
- X.-F. Yan, H.-M. Xiao, X.-D. Gong, X.-H. Ju, A comparison of semiempirical and first principle methods for establishing toxicological QSARs of nitroaromatics, *J. Mol. Struct. Theoret. Chem.* 764 (2006) 141–148.
- S. Karabulut, N. Sizochenko, A. Orhan, J. Leszczynski, A DFT-based QSAR study on inhibition of human dihydrofolate reductase, *J. Mol. Graph. Model.* 70 (2016) 23–29.
- S. Zare, M. Fereidoonzhad, D. Afshar, Z. Ramezani, A comparative QSAR analysis and molecular docking studies of phenyl piperidine derivatives as potent dual NK1R antagonists/serotonin transporter (SERT) inhibitors, *Comput. Biol. Chem.* 67 (2017) 22–37.
- K. Roy, S. Kar, R.N. Das, Statistical Methods in QSAR/QSPR, A Primer on QSAR/QSPR Modeling, (2015), pp. 37–59.
- J.G. Topliss, R.P. Edwards, Chance factors in studies of quantitative structure-activity relationships, *J. Med. Chem.* 22 (1979) 1238–1244.
- K.W. Thomulka, C.G. Abbas, D.A. Young, J.H. Lange, Evaluating median effective concentrations of chemicals with bioluminescent Bacteria, *Environ. Contam. Toxicol.* 56 (1996) 446–452.
- J. Zaldivar, L.O. Ingram, Effect of organic acids on the growth and fermentation of ethanogenic *Escherichia coli* LY01, *Biotechnol. Bioeng.* 66 (1999) 203–210.
- L. Su, X. Zhang, X. Yuan, Y. Zhao, D. Zhang, W. Qin, Evaluation of joint toxicity of nitroaromatic compounds and copper to *Photobacterium phosphoreum* and QSAR analysis, *J. Hazard. Mater.* 241–242 (2012) 450–455.
- C. Boillot, Y. Perrodin, Joint-action ecotoxicity of binary mixtures of glutaraldehyde and surfactants used in hospitals: use of the Toxicity Index model and isoblogram representation, *Ecotoxicol. Environ. Saf.* 71 (2008) 252–259.
- S. Broderius, M. Kahl, Acute toxicity of organic chemical mixtures to the fathead minnow, *Aquat. Toxicol.* 6 (1985) 307–322.
- S.J. Broderius, M.D. Kahl, M.D. Hoglund, Use of joint response to define the primary mode of toxic action for diverse industrial organic chemicals, *Environ. Toxicol. Chem.* 14 (1995) 1591–1605.
- L. Wang, W. Zou, Y. Zhong, J. An, X. Zhang, M. Wu, Z. Yu, The hormesis effect of BDE-47 in HepG2 cells and the potential molecular mechanism, *Toxicol. Lett.* 209 (2012) 193–201.
- J.R.M. Almeida, T. Modig, A. Petersson, B. Hahn-Hägerdal, G. Lidén, M.F. Gorwa-Grauslund, Increased tolerance and conversion of inhibitors in lignocellulosic hydrolysates by *Saccharomyces cerevisiae*, *J. Chem. Technol. Biotechnol.* 82 (2007) 340–349.
- Z.L. Liu, M. Ma, Comparative transcriptome profiling analyses during the lag phase uncover YAP1, PDR1, PDR3, RPN4, and HSF1 as key regulatory genes in genomic adaptation to the lignocellulose derived inhibitor HMF for *Saccharomyces cerevisiae*, *BMC Genomics* 11 (2010) 660.
- B. Hahn-Hägerdal, E. Palmqvist, Fermentation of lignocellulosic hydrolysates. II: inhibitors and mechanisms of inhibition, *Bioresour. Technol.* 74 (2000) 25–33.
- D.-L. Wang, Y.-L. Wu, E.-H. Guo, S. Song, J.-T. Feng, X. Zhang, Synthesis and QSAR study of novel  $\alpha$ -methylene- $\gamma$ -butyrolactone derivatives as antifungal agents, *Bioorg. Med. Chem. Lett.* 27 (2017) 1284–1290.
- R. Lin, J. Cheng, L. Ding, W. Song, J. Zhou, K. Cen, Inhibitory effects of furan derivatives and phenolic compounds on dark hydrogen fermentation, *Bioresour. Technol.* 196 (2015) 250–255.
- J. Andary, J. Maalouly, R. Ouaini, H. Chebib, M. Beyrouthy, D.N. Rutledge, N. Ouaini, Phenolic compounds from diluted acid hydrolysates of olive stones: effect of overliming, *Adv. Crop. Sci. Technol.* 1 (2016) 2329–8863.
- H.B. Klinke, A.B. Thomsen, B.K. Ahring, Inhibition of ethanol-producing yeast and bacteria by degradation products produced during pre-treatment of biomass, *Appl. Microbiol. Biotechnol.* 66 (2004) 10–26.
- H. Gu, J. Zhang, J. Bao, Inhibitor analysis and adaptive evolution of *Saccharomyces cerevisiae* for simultaneous saccharification and ethanol fermentation from industrial waste corn cob residues, *Bioresour. Technol.* 157 (2014) 6–13.
- R. Gómez-Bombarelli, M.T. Pérez-Prior, M.I. González-Sánchez, E. Valero, Biocatalytic oxidation of phenolic compounds by bovine methemoglobin in the presence of H<sub>2</sub>O<sub>2</sub>: quantitative structure–activity relationships, *J. Hazard. Mater.* 241–242 (2012) 207–215.
- Y. Liu, Y. Nie, J. Wang, J. Wang, X. Wang, S. Chen, G. Zhao, L. Wu, A. Xu, Mechanisms involved in the impact of engineered nanomaterials on the joint toxicity with environmental pollutants, *Ecotoxicol. Environ. Saf.* 162 (2018) 92–102.